Viscoelastic Fitzhugh-Nagumo models

D. Bini
Istituto per le Applicazioni del Calcolo "M. Picone," CNR, I-00161 Rome, Italy and International Center for Relativistic Astrophysics – I.C.R.A., University of Rome "La Sapienza," I-00185 Rome, Italy

C. Cherubini and S. Filippi
Facoltá di Ingegneria, Università Campus Biomedico, Via E. Longoni 83, I-00155 Roma, Italy and International Center for Relativistic Astrophysics – I.C.R.A., University of Rome "La Sapienza," I-00185 Rome, Italy
(Received 27 April 2005; published 27 October 2005)

An extended Fitzhugh-Nagumo model including linear viscoelasticity is derived in general and studied in detail in the one-dimensional case. The equations of the theory are numerically integrated in two situations: (i) a free insulated fiber activated by an initial Gaussian distribution of action potential, and (ii) a clamped fiber stimulated by two counter phased currents, located at both ends of the space domain. The former case accounts for a description of the physiological experiments on biological samples in which a fiber contracts because of the spread of action potential, and then relaxes. The latter case, instead, is introduced to extend recent models discussing a strongly electrically stimulated fiber so that nodal structures associated on quasistanding waves are produced. Results are qualitatively in agreement with physiological behavior of cardiac fibers. Modifications induced on the action potential of a standard Fitzhugh-Nagumo model appear to be very small even when strong external electric stimulations are activated. On the other hand, elastic backreaction is evident in the model.

DOI: 10.1103/PhysRevE.72.041929 PACS number(s): 87.19.Rr, 87.19.Nn, 87.10.+e, 05.45.−a

I. INTRODUCTION

Sudden cardiac death [1,2] as well as various cardiac arrhythmias have been evidenced—either experimentally or theoretically—to be related on reentrant waves of electrical activity [3–5] and in particular on rotating spiral waves of excitation [4,6,7]. Cardiac arrest in ventricular fibrillation is due to a compromised mechanical pump activity of the heart muscle. Cardiac contraction, in fact, is physiologically started by an electrical depolarization. However, in pathologic cases, this can be desynchronized by turbulence, affecting in turn the mechanical activity. The spatiotemporal evolution of ventricular fibrillation is widely studied using imaging of blood perfused isolated hearts [8–10], but in order to obtain a quantitative understanding of these phenomena an accurate mathematical data analysis [11] and modeling [12,13] is necessary. Impressively, some discoveries concerning fibrillating hearts have been triggered by pure numerical computation based on simple models [14–18]. Today the study of spatiotemporal dynamics of arrhythmias in two-dimensional (2D) or 3D simple geometries, as well as in anatomically accurate models of the heart (see Ref. [19] and references therein) is at the center of many mathematical simulations. Most of the existing studies, however, do not take into account the active mechanical deformations of the heart, which have been shown in experiments to alter the electrical properties of myocytes [20] and play an important role in ventricular arrhythmias [21]. For this reason, a variety of computational models have been used to investigate the effects of electrical activity on the sequence of 3D ventricular contractions [22–25], but such models have not accounted for the effects of mechanoelectric feedback, notwithstanding some seminal works of the middle and late 1990s [26,27]. Only recently, have these models been improved in a more systematic way, offering some first quantitative results of the simulations [28]. Both Fitzhugh-Nagumo theory and finite elasticity are described by nonlinear equations. Therefore a 2D or 3D mechanoelectric numerical simulation will consume much in terms of computational resources. In particular, these coupled strongly nonlinear systems can be easily affected by errors associated on a low number of nodes or finite elements and nonsufficient numerical accuracy [29]. For this reason one should define specific indicators which will give a quantification of the numerical quality of the simulation. The aim of the present study is to develop a model sufficiently complete to include the main mechanisms involved in the excitation-contraction coupling, but sufficiently simple to be tractable from an analytical and numerical point of view. In this paper, a viscoelastic model of cardiac tissue is introduced and analyzed in order to capture the mechanical aspect of the heart contraction, which is neglected in most models (the emphasis is generally put instead only on the electric aspects of electric propagation). The model is intended to be simple, both for the mechanical and for the electric aspect. The latter is treated with the Fitzhugh-Nagumo description. The former is applied in the simplified one-dimensional case, by introducing only one deformation field. We extend a 3D Fitzhugh-Nagumo model including linear viscoelasticity and then proceed to a computational analysis in the context of cardiac muscle fibers. The developed model does not include, for simplicity, cardiac myocyte membrane kinetics. In fact, in our case there is no necessity to model the single cell ionic currents with the accuracy and complexity inherent in the biophysically based models. With a view to investigating phenomena on a larger spatial and temporal scale, several ionic current models have been developed that do not seek to model subcellular processes but only to provide an action potential at a minimal computa-

tional cost. The original Fitzhugh-Nagumo simplified cardiac myocyte model [30,31] belongs to this class, and it is based on the cubic excitation; in addition, it includes a recovery variable so both depolarization and repolarization can be modeled. In 1994, Rogers and McCulloch modified the original model to generate a more realistic action potential [32]. The velocity of the upstroke was increased, and the large hyperpolarization at the end of the recovery phase was removed. In 1996, this form of the already modified Fitzhugh-Nagumo model was further updated by Aliev and Panfilov [33]. They altered the equation which modeled the change of the recovery variable to provide a more realistic restitution period and to allow for reentrant phenomena. In the paper of Nash and Panfilov [28], an extension of the Aliev and Panfilov [33] model to include an approximation of the actively developed stress during contraction is proposed to investigate the effects of mechanical deformation on cardiac excitation and various types of reentrant activity. The computational framework employs electromechanical and mechanoelectric feedback to couple a three-variable Fitzhugh-Nagumo-type excitation-tension model to the nonlinear stress equilibrium equations, which govern large deformation hyperelasticity. Numerically, the coupled electromechanical model combines a finite difference method approach to integrate the excitation equations, with a Galerkin finite element method to solve the equations governing tissue mechanics. Because cardiac cells change length by up to 20% during a normal heart beat, the mechanical analysis based on finite deformation elasticity theory is realistic and necessary in a global study of the problem. On the other hand the simple approach of our work is an interesting and useful first step toward modeling muscle fiber contraction in space with an analytical theory less realistic but useful to explain the elementary physics processes involved. Our theoretical analysis of the interplay between viscoelasticity and electric dynamics in heart fibers may help to give a more detailed understanding of the complex effects of mechanical activity on cardiac excitation which is not completely understood. While we do not consider detailed models of cardiac electromechanical wave propagation, our results may apply to some more elementary and fundamental aspects that must be observed in realistic models of the whole heart.

In this paper, the equations of the theory in one dimension will be numerically integrated in two situations: (i) a free insulated fiber activated by an initial Gaussian distribution of action potential, and (ii) a clamped fiber stimulated by two currents in counter phase located at both ends of the domain. The former case gives a reasonable description of the physiological experiments on biological samples in which a fiber contracts due to the spread of action potential and then relaxes. The latter case, nevertheless, is introduced with the aim to extend recent results of the literature. Results are qualitatively in agreement with physiological behavior of cardiac fibers, although the modifications induced on the action potential of standard Fitzhugh-Nagumo equations are very small and require strong external stimulations to be activated. On the other hand, elastic backreaction is evident in the model. As a last remark, we point out that the simulations are performed in the linear elastic case and in the simpler 1D regime due to the requirement of high accuracy and absence of causality violations. To this end, we will discuss the diagnostic of the codes in order to test the numerical integration. We aim, in this way, to be in accordance with the choice of numerical communities, primarily with modern numerical general relativity [34].

II. VISCOELASTIC FITZHUGH-NAGUMO MODELS: GENERAL THEORY

Cardiac cells are both excitable and contractile. They are excitable, enabling action potentials to propagate, and the action potential causes the cells to contract, thereby enabling the pumping of blood. The spread of excitation in the heart occurs due to excitability of individual cardiac cells as well as to close electrical coupling of cardiac cells via specialized contacts (gap junctions), through which depolarized cardiac cells can elicit excitation in neighboring cells, resulting in a propagation wave of activity. Thus models that describe propagation in the heart generally consist of two parts: a model of the cardiac cell, and a model describing cellular interconnections. In general, excitation of a cardiac cell is brought about by the change in potential across the cell membrane, due to transmembrane fluxes of various charged ions (Na^+, K^+, Ca_2^+, Cl^-, etc.). A reasonable mathematical description of these processes is based on the following equation [35]:

$$I = C_m \frac{dV}{dt} + I_m, \tag{1}$$

where I represents the total transmembrane current, C_m is the membrane capacitance, V is the transmembrane potential, and I_m is the ionic transmembrane current. To describe the time course of excitation of a single cardiac cell in the absence of external currents, one can solve Eq. (1) with $I=0$. To describe wave propagation in cardiac tissue, instead, it is necessary to specify the currents resulting from the intercellular coupling, which can usually be approximated as a cablelike equation:

$$I = \nabla \cdot (D \nabla V) \equiv \frac{\partial}{\partial x_k}\left(D_{ik} \frac{\partial}{\partial x_i} V \right), \tag{2}$$

where D is a tensor of conductivities, and ∇ is the gradient operator. Equation (2), taken together with appropriate descriptions of the transmembrane ionic currents (I_m), constitutes a model for the electrical properties of a cardiac tissue. In the classical Fitzhugh-Nagumo, one has a simplified model of the cell membrane, in which the cell consists of three components, a capacitor representing the membrane capacitance, a nonlinear current-voltage device for the fast current, and a resistor, inductor, and battery in series for the recovery current [35]. Mathematically one has

$$I_m = F(V) + i + I_0, \tag{3}$$

where I_0 is an applied external current, i is a gating current, and $F(V)$ is a cubic function of the potential. This function is chosen so that equation $F(V)=0$ admits three real roots located at $V=0$, $V=\alpha V_1$, and $V=V_1$, with $\alpha \in (0,1)$ being a real number. Therefore while the values of the potential

$V=0$ and $V=V_1>0$ correspond to stable solutions of the differential equation

$$C_m\frac{dV}{dt}=-F(V), \tag{4}$$

the constant α causes the remaining (unstable) solution, i.e., $V=\alpha V_1$, to be located in between.

A typical choice for $F(V)$ is then

$$F(V)=-\frac{V}{\alpha R_1}\left(1-\frac{V}{V_1}\right)\left(\frac{V}{V_1}-\alpha\right), \tag{5}$$

with $R_1=1/F'(0)$ so that Eq. (1) assumes the form

$$\boldsymbol{\nabla}\cdot(D\,\boldsymbol{\nabla}\,V)=C_m\frac{dV}{dt}+F(V)+i+I_0. \tag{6}$$

This equation is coupled to the current circulation equation

$$L\frac{\partial i}{\partial t}+Ri=V-V_0, \tag{7}$$

where V is the membrane potential, V_0 is a potential gain across the battery, and R and L are the resistance and the inductance of the membrane. The coupled equations (6) and (7) are enough to describe propagation of electric signals over a cardiac tissue.

The elastic deformation and viscosity of the cardiac tissue are well known, we are therefore motivated to extend a Fitzhugh-Nagumo model including elasticity (linear elasticity in this paper) and viscosity. Concerning elastic deformations, the starting point is the relation of every point of a body x_i, which due to deformations reaches a new position x_i' related to the old one by $x_i'=x_i+u_i$, with u_i being the deformation or relative displacement vector. The fundamental equation is then Newton's law for an isotropic solid medium with viscoelasticity in interaction with an electric field [36,37]:

$$\rho\frac{\partial^2 u_i}{\partial t^2}=\frac{\partial\sigma_{ik}}{\partial x_k}, \tag{8}$$

with

$$\sigma_{ik}=\sigma_{ik}^{(0)}+\sigma_{ik}'^{(0)}+\frac{2\varepsilon_0-a_1}{8\pi}\mathcal{E}_i\mathcal{E}_k-\frac{\varepsilon_0+a_2}{8\pi}\mathcal{E}_j^2\delta_{ik}, \tag{9}$$

where the quantity $\mathcal{E}_i$ in Eq. (9) represents the electric field which is related to external potential via $\mathcal{E}_i=-\partial V/\partial x_i$. Moreover, here $\sigma_{ik}^{(0)}$ is the stress tensor in absence of electric interactions, i.e.,

$$\sigma_{ik}^{(0)}=\frac{E}{1+\lambda}\left(u_{ik}+\frac{\lambda}{1-2\lambda}u_{ll}\delta_{ik}\right), \tag{10}$$

with $u_{ik}=\frac{1}{2}(\partial u_i/\partial x_k+\partial u_k/\partial x_i)$ (linear elasticity deformation tensor) and $\sigma_{ik}'^{(0)}$ is the viscous contribution

$$\sigma_{ik}'^{(0)}=2\eta\left(\frac{\partial u_{ik}}{\partial t}-\frac{1}{n}\delta_{ik}\frac{\partial u_{ll}}{\partial t}\right)+\zeta\frac{\partial u_{ll}}{\partial t}\delta_{ik}, \tag{11}$$

where n is the space dimension ($n=3$ in ordinary Euclidean space). Moreover, E is Young's modulus, λ is Poisson's coefficient, ε_0 is the dielectric permittivity of the undeformed body, and the constants a_1 and a_2 come, following Landau's treatment, from the most general linear expression of the dielectric tensor in terms of u_{ik}, i.e.,

$$\varepsilon_{ik}=\varepsilon_0\delta_{ik}+a_1u_{ik}+a_2u_{ll}\delta_{ik}. \tag{12}$$

Finally, ρ is the mass density of the body, while η and ζ are two positive viscosity coefficients. In Fitzhugh-Nagumo equations (6) and (7), we use D_{ik} (with dimensions of $[\text{length}]^2\times[\text{resistance}]^{-1}$), expanded analogously as the dielectric tensor, i.e.,

$$D_{ik}=D_0\delta_{ik}+b_1u_{ik}+b_2u_{ll}\delta_{ik}, \tag{13}$$

which couples such equations with Eq. (8), defining in this way a viscoelastic Fitzhugh-Nagumo model, so then contraction and extension of the medium backreacts with its electric properties. In the following we specialize this model to the 1D case, with the aim to model a heart fiber whose length results in being larger than its section.

III. ONE-DIMENSIONAL CASE

We are primarily interested in the propagation of longitudinal (compressional) waves in the elastic medium, i.e., $u_i=u_i(t,x)\equiv W(t,x)\delta_{i1}$ only. Hence, in one dimension, Eqs. (6), (7), and (8), collapse to

$$\frac{1}{c_l^2}\frac{\partial^2 W}{\partial t^2}-\frac{\partial^2 W}{\partial x^2}=\frac{\zeta}{\rho}\frac{\partial^3 W}{\partial t\,\partial x^2}+\left(\frac{\varepsilon_0-(a_1+a_2)}{4\pi\rho}\right)\frac{\partial V}{\partial x}\frac{\partial^2 V}{\partial x^2},$$

$$C_m\frac{\partial V}{\partial t}+F(V)+i+I_0=\left[D_0+(b_1+b_2)\frac{\partial W}{\partial x}\right]\frac{\partial^2 V}{\partial x^2}+(b_1+b_2)\frac{\partial V}{\partial x}\frac{\partial^2 W}{\partial x^2},$$

$$L\frac{\partial i}{\partial t}+Ri=V-V_0, \tag{14}$$

with $c_l=\sqrt{E(1-\lambda)/\rho(1+\lambda)(1-2\lambda)}$ is the (longitudinal) sound speed. It is useful to adimensionalize the equations above. This step is performed in the next subsection.

A. Adimensionalization

It is helpful to introduce the notation: $\varepsilon_0-(a_1+a_2)=\varepsilon_d$ and $b_1+b_2=D_1$. Let us proceed to determine a nondimensional form for the system (14). To this end we consider natural scale lengths for the electric potential (V_1) and the resistance (R_1) so that the length scale for currents is automatically defined (V_1/R_1). A time scale length can be defined using the self-induction coefficient and a natural space length is obtained by using the sound speed. Summarizing, using the following set of rescalings:

$$V(t,x) = V_1 v(t,x), \quad i(t,x) = \frac{V_1}{R_1} u(t,x), \quad t = \frac{L}{R_1} T, \quad x = \frac{c_l L}{R_1} X,$$

$$C_m = \frac{\varepsilon L}{R_1^2}, \quad I_0 = \frac{u_0 V_1}{R_1}, \quad V_0 = v_0 V_1, \quad R = \gamma R_1, \quad \zeta = \frac{L\rho}{R_1}\sigma,$$

$$D_0 = \frac{c_l^2 L^2}{R_1^3}\delta_0, \quad D_1 = \frac{c_l^3 L^3}{R_1^3}\delta_1, \quad \epsilon_d = \frac{4\pi c_l^2 L^2 \rho}{R_1^2 V_1^2} E_d,$$

$$W(t,x) = \frac{c_l L}{R_1} w(t,x), \tag{15}$$

we get the nondimensional version of Eq. (14),

$$\frac{\partial^2 w}{\partial T^2} - \frac{\partial^2 w}{\partial X^2} = \sigma \frac{\partial^3 w}{\partial T\, \partial X^2} + E_d \frac{\partial v}{\partial X}\frac{\partial^2 v}{\partial X^2},$$

$$\epsilon \frac{\partial v}{\partial T} = \frac{1}{\alpha} v(1-v)(v-\alpha) - u - u_0 + \left[\delta_0 + \delta_1 \frac{\partial w}{\partial X}\right]\frac{\partial^2 v}{\partial X^2} + \delta_1 \frac{\partial v}{\partial X}\frac{\partial^2 w}{\partial X^2},$$

$$\frac{\partial u}{\partial T} = v - v_0 - \gamma u. \tag{16}$$

In order to compare our results with recent literature on the subject [38], it is illustrative to rearrange terms as follows: we introduce the new time variable $T=\alpha\epsilon\tau$ and rescale the u variable as $u(\tau,X)=\mathcal{U}(\tau,X)/\alpha$; hence $u_0=\mathcal{U}_0/\alpha$ and for convenience we set $v=\mathcal{V}$ and $v_0=\mathcal{V}_0$. Then, we introduce the following notation:

$$\gamma = a\alpha, \quad \epsilon = e_1/\alpha^2, \quad \sigma = s\alpha/e_1, \quad E_d = e_2\alpha^2/e_1^2,$$

$$\delta_0 = D/\alpha, \quad \delta_1 = D_1/\alpha, \quad \mathcal{U}_0 = -I_{\text{ext}}. \tag{17}$$

In this way system (16) becomes

$$\frac{\partial^2 w}{\partial \tau^2} - \frac{e_1^2}{\alpha^2}\frac{\partial^2 w}{\partial X^2} = s\frac{\partial^3 w}{\partial \tau\, \partial X^2} + e_2 \frac{\partial \mathcal{V}}{\partial X}\frac{\partial^2 \mathcal{V}}{\partial X^2},$$

$$\frac{\partial \mathcal{V}}{\partial \tau} = \mathcal{V}(1-\mathcal{V})(\mathcal{V}-\alpha) - \mathcal{U} + I_{\text{ext}} + \left[D + D_1\frac{\partial w}{\partial X}\right]\frac{\partial^2 \mathcal{V}}{\partial X^2} + D_1 \frac{\partial \mathcal{V}}{\partial X}\frac{\partial^2 w}{\partial X^2},$$

$$\frac{\partial \mathcal{U}}{\partial \tau} = e_1(\mathcal{V} - a\mathcal{U} - \mathcal{V}_0), \tag{18}$$

and this is the final form of equations which describe propagation of coupled interacting "electroviscoelastic signals" which will be numerically integrated in the following.

B. Advanced and retarded solutions

Equations (18) admit purely advanced or retarded solutions. In fact, passing to coordinates $\xi=X+(e_1/\alpha)\tau$ and $\eta=X-(e_1/\alpha)\tau$ and looking for special solutions of the form $w=w(\eta)$, $\mathcal{V}=\mathcal{V}(\eta)$, $\mathcal{U}=\mathcal{U}(\eta)$, $I_{\text{ext}}=0$, for example, we obtain the first order autonomous ordinary differential equation (ODE) system:

$$\dot{\mathcal{V}} = Y,$$

$$\dot{w} = M,$$

$$\dot{M} = -\frac{\alpha e_2}{2 s e_1}(C - Y^2),$$

$$\dot{\mathcal{U}} = \alpha(\mathcal{V}_0 + a\mathcal{U} - \mathcal{V}),$$

$$\dot{Y} = \frac{1}{D + D_1 M}\left\{\mathcal{U} + \mathcal{V}(\mathcal{V}-1)(\mathcal{V}-\alpha) - \frac{Y[D_1\alpha^2 e_2(Y^2 - K) + 2e_1^2 s]}{2\alpha s e_1}\right\}, \tag{19}$$

where the dot means ordinary differentiation with respect to the η parameter. For solutions depending by η only, the procedure is analogous. The quantity K is an integration constant, obtained reducing by quadrature one of the ODEs. It can be easily shown that equilibrium points of the dynamical system (19) exist if $K=0$ only. In this case $Y=0$, $M=0$, leading to

$$\mathcal{V}_0 + a\mathcal{U} - \mathcal{V} = 0, \quad \mathcal{U} + \mathcal{V}(\mathcal{V}-1)(\mathcal{V}-\alpha) = 0 \tag{20}$$

which coincides with the equilibrium position of the standard (nonelastic) Fitzhugh-Nagumo model.

IV. NUMERICAL ANALYSIS

In order to numerically integrate the system of second order partial differential equations [PDEs] (18), it is convenient to transform it in a first order one as follows:

$$\frac{\partial w}{\partial \tau} = P,$$

$$\frac{\partial P}{\partial \tau} = \frac{\partial}{\partial X}\left[\frac{e_1^2}{\alpha^2}\frac{\partial w}{\partial X} + s\frac{\partial P}{\partial X} + \frac{e_2}{2}\left(\frac{\partial \mathcal{V}}{\partial X}\right)^2\right],$$

$$\frac{\partial \mathcal{V}}{\partial \tau} = \frac{\partial}{\partial X}\left[D\frac{\partial \mathcal{V}}{\partial X} + D_1\frac{\partial \mathcal{V}}{\partial X}\frac{\partial w}{\partial X}\right] + \mathcal{V}(1-\mathcal{V})(\mathcal{V}-\alpha) - \mathcal{U} + I_{\text{ext}},$$

$$\frac{\partial \mathcal{U}}{\partial \tau} = e_1(\mathcal{V} - a\mathcal{U} - \mathcal{V}_0). \tag{21}$$

This step automatically generates a constraint $C=|P-\partial w/\partial\tau|$, which in the exact theory is identically zero but will not vanish in a general numerically approximated solution. Deviations of this quantity from zero clearly provide a useful indicator of the quality of the numerical results, i.e., "causality violations" due to numerical modifications of

the characteristics of the PDE system. In fact, such violations will instantaneously propagate through the domain of integration, leading to nonphysical results. In the numerical simulations we have kept C below a typical threshold of $\sim 10^{-4}$. The system of four coupled first order PDEs is numerically solved in the spatial domain $X \in [0,L]$, using the nonlinear finite element engine of FEMLAB® with fifth order Hermite elements. We acknowledge that existing models in the literature typically use dimensionless units whereas simulation results are often compared to dimensional observations from experimental studies. To this end, dimensional mappings are obtained by comparing specific dimensionless model properties with experimental data [28]. This inductive procedure in general allows us to bypass working directly with physical constants. We have performed the following typical choice of numerical parameters:

$$L = 5, \quad e_1 = 0.01, \quad \alpha = 0.1, \quad a = 2.5, \quad D = 1, \quad \mathcal{V}_0 = 0, \tag{22}$$

following Ref. [38], which contains, moreover, a discussion on the conversion relations with physical scales.

Concerning the remaining parameters, some approximate estimations can be done as follows. Equation (18), for the elastic deformations, has an effective source term represented by the derivatives of the action potential. When such term is absent ($e_2=0$), one can estimate the effect of the viscous parameter s looking for solutions of the form $w = w_0 e^{ikX - i\omega\tau}$, where $\omega = \omega_0 + i\omega_1$, k being the wave number of the solution and $\omega_0 = \pm(k/2\alpha)\sqrt{4e_1^2 - k^2\alpha^2 s^2}$, $\omega_1 = -sk^2/2$. Such a dispersion relation implies that $s > 2e_1/k\alpha$. With the parameters listed in Eq. (22), assuming $k = 2\pi/L$, we obtain $s > 0.16$ which identifies a typical scale of this parameter.

Regarding e_2, we can have an estimate looking for static solutions of Eq. (18), in which the action potential is approximated by a quadratic polynomial function $\mathcal{V} = (h/2)X^2$, leading to a linear electric field and representing consequently the simplest possible test field. In $X = L$, we have $\mathcal{V}(L) = (h/2)L^2$, so that, taking into account that for a Fitzhugh-Nagumo model in our adimensionalized variables the maximum voltage $\mathcal{V}_{\max} \simeq 0.8$, we choose $\mathcal{V}(L) \simeq \mathcal{V}_{\max}/2$. We require, moreover, that w and its first spatial derivative vanish at $X=0$ and hence one finds $w(X) = -(\alpha^2 h^2 e_2/6e_1^2)X^3$. We require that $|w(L)/L| \simeq 0.05$ in order to have linear elasticity conditions being satisfied. With the above choice of parameters we get $e_2 \simeq 0.2$. Concerning D_1 unfortunately similar simple arguments do not apply. We are then forced to suppose that the total effective diffusion coefficient $D + D_1 \partial_X w$ must not differ very much from the nonelastic one D. Consequently we will perform a reasonable choice for D_1 with values smaller or around the value of D.

We present now two different situations: (i) a free insulated fiber activated by an initial Gaussian distribution of action potential, and (ii) a clamped fiber stimulated by two counter phased currents, located at both ends of the space domain.

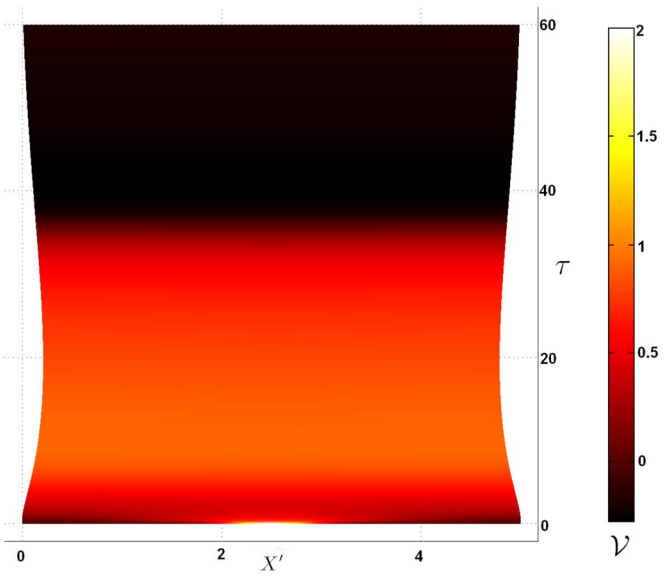

FIG. 1. (Color online) Density plot of $\mathcal{V}$ in the plane $X' = X + w$ (abscissa) and τ (ordinate). The shaded scale defines the value of $\mathcal{V}$.

A. Free fiber

In this case we adopt for system (21) the following choice of parameters:

$$D_1 = 1.5, \quad e_2 = 0.3, \quad s = 0.2, \tag{23}$$

in addition to Eq. (22). We require, moreover, $I_{\text{ext}}=0$ and we set as initial data $w = \mathcal{U} = 0$ and $\mathcal{V} = Je^{-r(X-L/2)^2}$ with $J=2$ and $r=5$. Given a point X at $\tau=0$, its (adimensional) position during the dynamics will be $X' = X + w(\tau, X)$. Concerning boundary conditions we use Neumann zero flux ones, i.e.

$$\frac{\partial \mathcal{U}}{\partial X} = \frac{\partial \mathcal{V}}{\partial X} = \frac{\partial w}{\partial X} + \frac{s\alpha^2}{e_1^2}\frac{\partial P}{\partial X} = 0$$

both in $X=0$ and $X=L$. In Fig. 1 we show a density plot of $\mathcal{V}$ in the plane $X' = X + w$ (abscissa) and τ (ordinate). The shaded scale defines the value of $\mathcal{V}$. Lighter gray means high value of the action potential, dark gray means lower action potential. As expected the fiber contracts with respect to its position at rest, due to the action potential spreading. Once action potential disappears the fiber returns back to its original length. This evolution is also shown at different times in plane $(X', \mathcal{V})$ in Fig. 2. Changing the sign for e_2, one gets that the fiber will expand instead of contracting.

In Fig. 3 we present instead, the quantity $\mathcal{V}$ (the action potential) in function of τ taken in $X=1$, both in the elastic case (dotted) and the nonelastic standard Fitzhugh-Nagumo one (continuous curve). We easily realize that electric activity in this case is not affected by elasticity, although elasticity is clearly activated by $\mathcal{V}$.

In Fig. 4 we plot the adimensionalized displacement w of the point initially located in $X=1$ in function of τ. As expected the point $X=1$ is pushed towards the center of the fiber and then comes back to its rest position when $w \to 0$ at late times. This behavior agrees with standard physiological experiments on elastic heart fibers.

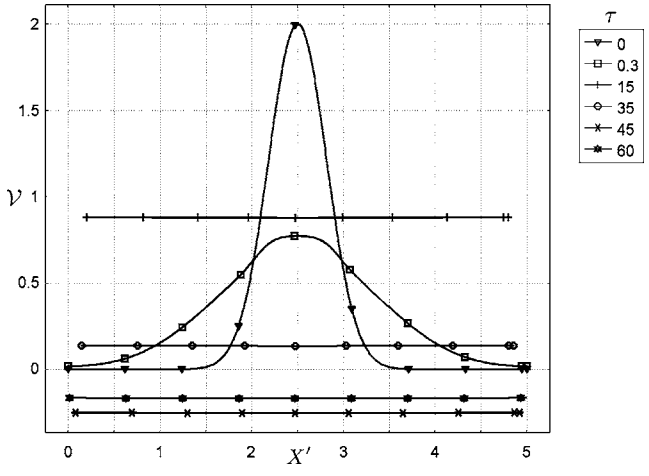

FIG. 2. Plot of $\mathcal{V}$ against $X'=X+w$ at different values of $\tau=0$, 0.3, 15, 35, 45, 60.

In Fig. 5 we show the value of the constraint C at various "time scales" of the numerical simulation. As anticipated, causality violations result very small making the integration meaningful. Similar "error bars" are not usually presented in the literature, although such a discussion is essential to have a clear understanding of the soundness of a numerical simulation. In relation with the accuracy problem, we point out that our numerical integrations have been carefully checked against numerical violations of imposed boundary conditions too. In fact, in order to maintain zero flux Neumann conditions (or null Dirichlet conditions, as discussed in the following) below the reasonable threshold of $\sim 10^{-8}$ during the evolution, we had to use many finite elements, a procedure which, in one-dimensional systems, can be still performed. In higher dimensions, however, boundary and constraint violations can surely represent a serious problem, and clearly they must be reduced by implementation of an advanced constrained evolution scheme, together with a very fine meshing of the spatiotemporal integration domain. Presently, these constrained techniques exist in a well-developed form,

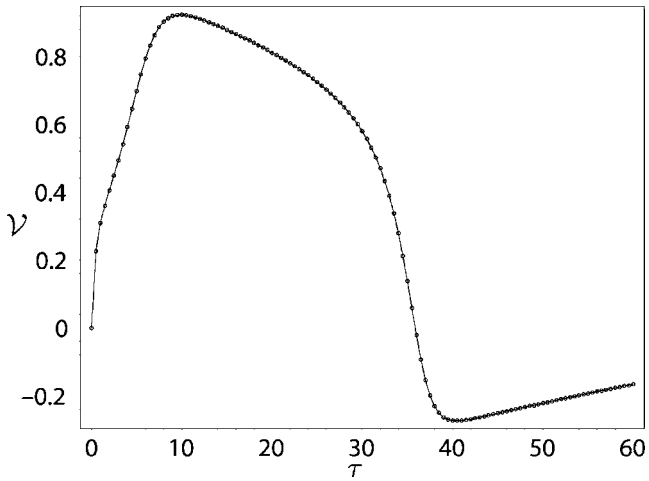

FIG. 3. Plot of the quantity $\mathcal{V}$ (the action potential) in function of τ taken in $X=1$, both in the elastic case (dotted) and the nonelastic one (continuous curve).

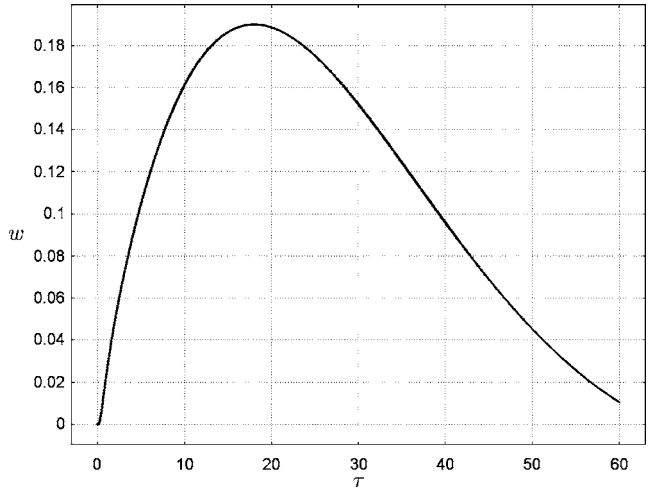

FIG. 4. Plot the adimensionalized displacement w of the point initially located in $X=1$ in a function of τ.

at the moment, for strongly hyperbolic problems and have been adopted, for instance, in numerical general relativity [34] to prevent the generation of nonphysical signals by boundary conditions violation. In future projects, passing to 1D nonlinear elasticity as well as to 2D and 3D linear cases, we will try to adapt such useful tools to elastic reaction-diffusion problems too, in order to have under control long time evolutions of models (especially if large elastic deformations will be considered) and be able to maintain C below lower thresholds.

B. Clamped stimulated fiber

In this section we extend the results of Ref. [38], based on experiments on real animal hearts electrically stimulated by external currents [39]. We consider now in system (21) a couple of external currents with functional form

$$I_{\text{ext}}(\tau,X) = B\sin(2\pi f\tau)e^{-\lambda X^2} + B\sin(2\pi f\tau+\phi)e^{-\lambda(X-L)^2}, \tag{24}$$

which for large values of λ will be practically located at both ends of the fiber. Following Ref. [38] again, we set

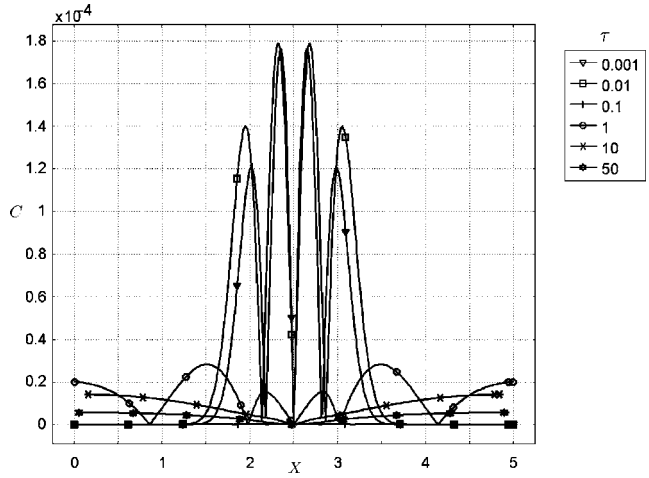

FIG. 5. Value of the constraint C at various "time scales" of the numerical simulation.

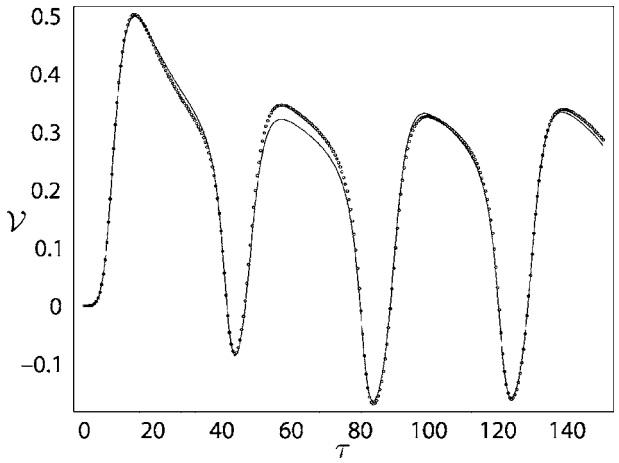

FIG. 6. Plot of the quantity $\mathcal{V}$ (the action potential) in function of time τ. The signal is taken in the middle of the fiber in the elastic case (dotted) and the nonelastic one (continuous curve).

$$\phi = \pi, \quad \lambda = 1000, \quad B = -30, \quad f = 0.0125. \tag{25}$$

Concerning the model parameters, we keep the same values of the free fiber case (22); we have tested a wide variety of choices for the remaining parameters in order to better understand their role in the dynamics. Here we study the case

$$D_1 = 0.36, \quad e_2 = -0.36, \quad s = 0.9, \tag{26}$$

which has manifested relevant changes with respect to the nonelastic case. The initial data are $\mathcal{U}=\mathcal{V}=w=0$ for $\tau=0$. The boundary conditions are zero flux Neumann ones for $\mathcal{U}$ and $\mathcal{V}$, i.e., $\partial\mathcal{U}/\partial X=\partial\mathcal{V}/\partial X=0$ both in $X=0$ and $X=L$. Concerning the variable w and P, we use the null Dirichlet condition $w=P=0$ on the extremal points instead (fixed rod).

In Fig. 6 we present, superimposed, the quantity $\mathcal{V}$ (the action potential) in function of τ: the signal is taken in the middle of the fiber in the elastic case (dotted) and the nonelastic one (continuous curve). Due to the strong external electric stimulation, in this case we have that the action potential is noticeably modified with respect to the nonelastic case. In Fig. 7 we plot w with respect to X. The various parts

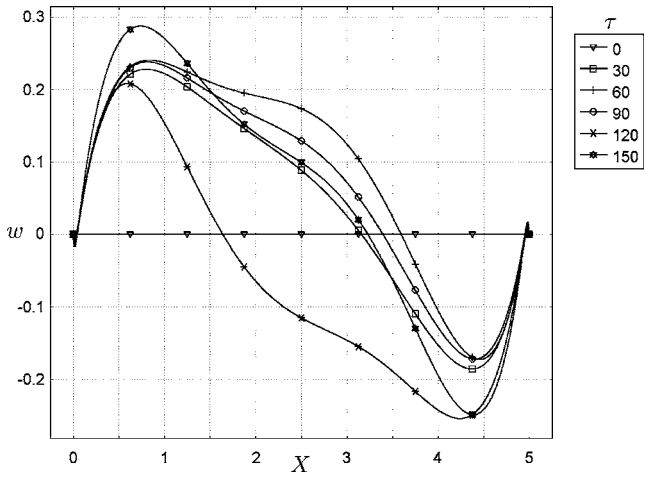

FIG. 7. Plot of w respect to X.

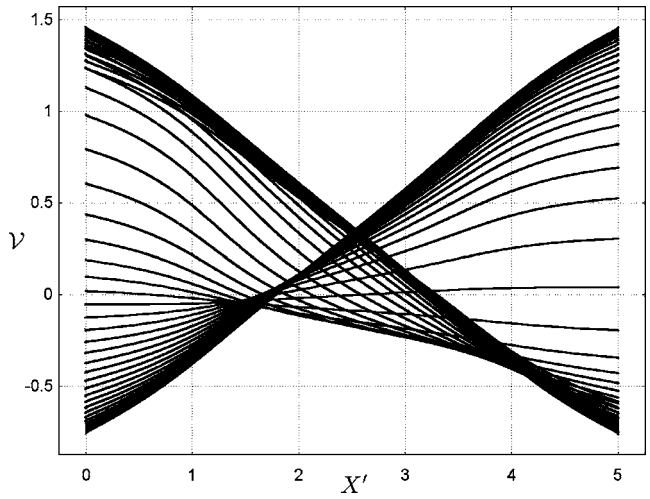

FIG. 8. Plot of the value of $\mathcal{V}$ with respect to X' at different values of τ, with $\tau \in [100,150]$.

of the fiber do not move relevantly with respect to the initial configuration, which is one of the conditions for which the linear elasticity condition results to be valid.

In Fig. 8 we plot the value of $\mathcal{V}$ with respect to X' at different values of τ, with $\tau \in [100,150]$. In Fig. 9 we plot the same quantity in the case of absence of elasticity (standard Fitzhugh-Nagumo model). Clearly, in both cases it appears at late times the central node of Ref. [38], whose position and amplitude are practically unaffected by the elastic addition. However, it must be noted that the elastic addition has slightly modified the behavior of the signals far from the center. These results clearly show that if one wants to change, or even to remove mechanically, the nodal structure, there should presumably used a nonlinear elastic theory with possible anisotropies.

The authors may wish to clarify this in their conclusions and perhaps consider the inclusion of stretch-activated channels and their associated mechanoelectric feedback as future work.

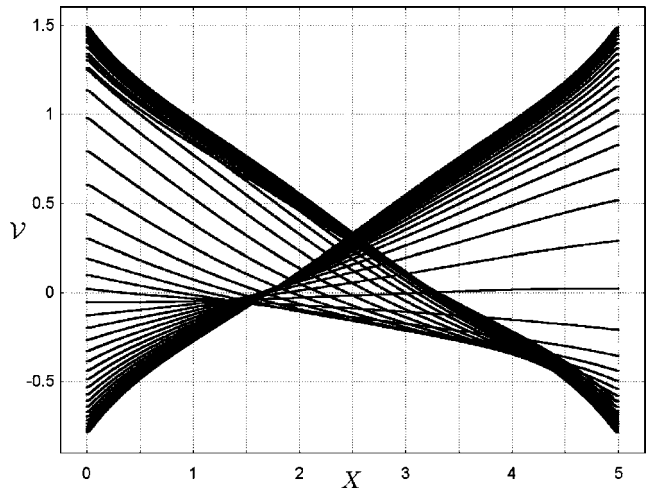

FIG. 9. Plot of the value of $\mathcal{V}$ with respect to X at different values of τ, with $\tau \in [100,150]$ in the absence of elasticity.

V. CONCLUSIONS

An extended Fitzhugh-Nagumo model including linear viscoelasticity has been derived and discussed. The equations of the model have been numerically integrated in two different one-dimensional situations: free fiber and an externally stimulated clamped one. The results are qualitatively in agreement with physiological behavior of cardiac fibers: we have found that, although elasticity is strongly affected by electric activity, the action potential does not backreact noticeably, unless the fiber is strongly electrically stimulated. In fact, modifications of action potential appear in experiments when a cardiac tissue is strongly stretched by external actions only [27,28].

In previous studies, which measured the effects of stretch on membrane potential, White *et al.* [40] found, according to experimental results regarding multicellular preparations [41], qualitatively and quantitatively variable membrane potential and action potential configurations depending upon sarcomere length changes. If the stretch increased sarcomere length from 1.84 to 2.70 μm the only parameter which changed was action potential duration which decreased. The primary mechanism behind such an effect seems to be stretch-activated channels, which open in response to stretch and produce an additional potassium transmembrane current that increases the speed of repolarization (see Ref. [42] for a recent review). The (nontrivial) inclusion of stretch-activated channels and their associated mechanoelectric feedback, not taken into account in this paper, will be addressed in future studies.

Moreover, we remark that in the extreme situation of a strong stretch one should clearly add to the elasticity equation the external mechanical forces which will activate these modifications and generate very large deformations. This, in principle, could be done, and it would require the use of the nonlinear elasticity theory (finite elasticity [36,43] including density variations) in which the strain tensor will contain an additional nonlinear term, i.e., $u_{ik}=\frac{1}{2}[\partial u_i/\partial x_k+\partial u_k/\partial x_i+(\partial u_l/\partial x_i)(\partial u_l/\partial x_k)]$. Such modification is nontrivial due to the possible presence of bifurcations in the nonlinear field equations [44]. Numerically, the problem will become much more complicated, requiring necessarily a more refined constrained evolution scheme. In future works, we will look for possible choices of parameters, which will best fit the experiments in laboratories on real heart fibers. At this stage, adopting the proper mathematical tools to have numerical simulations under control, the model presented in this paper will be generalized including nonlinear 1D elasticity and possibly adding heat transfer. Then, we will be ready to attack the problem in two or even three dimensions with the anticipation of being able to generate physiologically more realistic long term waveforms.

[1] R. J. Myerburg *et al.*, in *Cardiac Electrophysiology, From Cell to Bedside* (W.B. Saunders, Philadelphia, 1990).

[2] R. Pool, Science **247**, 1294 (1990).

[3] M. A. Allessie, F. I. M. Bonke, and F. J. G. Schopman, Circ. Res. **33**, 54 (1973).

[4] J. M. Davidenko, A. M. Pertsov, R. Salomonsz, W. T. Baxter, and J. Jalife, Nature (London) **355**, 349 (1992).

[5] L. Glass and M. E. Josephson, Phys. Rev. Lett. **75**, 2059 (1995).

[6] A. T. Winfree, J. Theor. Biol. **138**, 353 (1989).

[7] A. M. Pertsov, J. M. Davidenko, R. Salomonz, W. T. Baxter, and J. Jalife, Circ. Res. **72**, 631 (1993).

[8] R. A. Gray, A. M. Pertsov, and J. Jalife, Nature (London) **392**, 75 (1998).

[9] F. X. Witkowski, L. J. Leon, P. A. Penkoske, W. R. Giles, M. L. Spano, W. L. Ditto, and A. T. Winfree, Nature (London) **392**, 78 (1998).

[10] A. V. Holden, Nature (London) **392**, 20 (1998).

[11] A. L. Goldberger, L. A. N. Amaral, J. M. Hausdorff, P. C. Ivanov, C. K. Peng, and H. E. Stanley, Proc. Natl. Acad. Sci. U.S.A. **99**, 2463 (2002).

[12] G. K. Moe, W. C. Reinbolt, and J. A. Abildskov, Am. Heart J. **67**, 200 (1964).

[13] A. V. Panfilov and A. M. Pertsov, Philos. Trans. R. Soc. London, Ser. A **359**, 1315 (2001).

[14] A. T. Winfree, J. Biosci. **27**, 465 (2002).

[15] F. B. Gulko and A. A. Petrov, Biofizika **17**, 261 (1972).

[16] A. V. Panfilov and A. M. Pertsov, in *Autowave Processes in Systems with Diffusion* [Acad. Sci. USSR, Gorky, 1981), p. 77 (in Russian).

[17] V. S. Zykov, *Simulation of Wave Processes in Excitable Media* (Manchester University Press, Manchester, 1987).

[18] A. V. Panfilov and A. M. Pertsov, Dokl. Akad. Nauk SSSR **274**, 1500 (1984).

[19] D. J. Christini and L. Glass, Chaos **12**, 732 (2002).

[20] W. Sigurdson, A. Ruknudin, and F. Sachs, Am. J. Physiol. **262**, H1110 (1992).

[21] M. R. Franz, R. Cima, D. Wang, D. Profitt, and R. Kurz, Circulation **86**, 968 (1992).

[22] J. M. Guccione, K. D. Costa, and A. D. McCulloch, J. Biomech. **28**, 1167 (1995).

[23] M. P. Nash and P. J. Hunter, J. Elast. **61**, 113 (2000).

[24] T. P. Usyk, I. J. Le Grice, and A. D. McCulloch, Visual Comput. **4**, 249 (2002).

[25] R. C. P. Kerckhoffs, P. H. M. Bovendeerd, J. C. S. Kotte, F. W. Prinzen, K. Smits, and T. Arts, Ann. Biomed. Eng. **31**, 536 (2003).

[26] P. J. Hunter, M. P. Nash, and G. B. Sands, in *Computational Biology of the Heart*, edited by A. V. Panfilov and A. V. Holden (Wiley, West Sussex, England, 1997), Chap. 12, p. 345.

[27] P. Pelce, J. Sun, and C. Langeveld, Chaos, Solitons Fractals **5**, 383 (1995).

[28] M. P. Nash and A. V. Panfilov, Prog. Biophys. Mol. Biol. **85**, 501 (2004).

[29] T. J. R. Hughes, *The Finite Element Method: Linear Static and Dynamic Finite Element Analysis* (Dover, New York, 2000).

[30] R. A. Fitzhugh, Biophys. J. **1**, 445 (1961).
[31] J. Nagumo, S. Animoto, and S. Yoshizawa, Proc. Inst. Radio Engineers **50**, 2061 (1962).
[32] J. M. Rogers and A. D. McCulloch, IEEE Trans. Biomed. Eng. **41**, 743 (1994).
[33] R. R. Aliev and A. V. Panfilov, Chaos, Solitons Fractals **7**, 293 (1996).
[34] M. A. Scheel, A. L. Erickcek, L. M. Burko, L. E. Kidder, H. P. Pfeiffer, and S. A. Teukolsky, Phys. Rev. D **69**, 104006 (2004).
[35] J. Keener and J. Sneyd, *Mathematical Physiology* (Springer, New York, 1998).
[36] A. M. Kosevich, E. M. Lifshitz, L. D. Landau, and L. P. Pitaevskii, *Course of Theoretical Physics: Theory of Elasticity*, 3rd ed. (Butterworth-Heinemann, Washington, DC, 1986), Vol. 7.
[37] E. M. Lifshitz, L. D. Landau, and L. P. Pitaevskii, *Course of Theoretical Physics: Electrodynamics of Continuous Media*, 2nd ed. Butterworth-Heinemann, Washington, DC, 1984), Vol. 8.
[38] S. Takagi, A. Pumir, L. Kramer, and V. Krinsky, Phys. Rev. Lett. **90**, 124101 (2003).
[39] R. A. Gray, O. A. Mornev, J. Jalife, O. V. Aslanidi, and A. M. Pertsov, Phys. Rev. Lett. **87**, 168104 (2001).
[40] E. White, J. Y. Le Guennee, J. M. Nigretto, F. Gannier, J. A. Argibay, and D. Garnier, Exp. Physiol. **78**, 65 (1993).
[41] M. J. Lab, D. G. Allen, and C. H. Orchard, Circ. Res. **55**, 825 (1984).
[42] F. B. Sachse, *Computational Cardiology* (Springer-Verlag, Berlin, 2004).
[43] A. E. Green and W. Zerna, *Theoretical Elasticity*, 2nd ed. (Dover, New York, 2002).
[44] J. E. Marsden and T. J. R. Hughes, *Mathematical Foundations of Elasticity* Dover, New York, 1994).